Received: 5 November 2021 | Revised: 29 June 2022 | Accepted: 1 July 2022

DOI: 10.1002/jmor.21495

RESEARCH ARTICLE

JOURNAL OF morphology WILEY

The relationship between hard and soft tissue structures of the eye in extant lizards

Momo Yamashita[1,2] | Takanobu Tsuihiji[3,4]

[1]Center for Collections, National Museum of Nature and Science, Tsukuba, Ibaraki, Japan

[2]Geological Survey of Japan, National Institute of Advanced Industrial Science and Technology (AIST), Tsukuba, Ibaraki, Japan

[3]Department of Geology and Paleontology, National Museum of Nature and Science, Tsukuba, Ibaraki, Japan

[4]Department of Earth and Planetary Science, The University of Tokyo, Tokyo, Japan

Correspondence

Momo Yamashita, Center for Collections, National Museum of Nature and Science, 4-1-1, Amakubo, Tsukuba, Ibaraki 305-0005, Japan.
Email: myamashita@kahaku.go.jp

Funding information

Academist, Grant/Award Number: https://academist-cf.com/projects/8; Japan Society for the Promotion of Science, Grant/Award Number: KAKENHI 15J10919

Abstract

The sizes of the eye structures, such as the lens diameter and the axial length, are important factors for the visual performance and are considered to be related to the mode of life. Although the size of these soft structures cannot be directly observed in fossil taxa, such information may be obtained from measuring size and morphology of the bony scleral ossicle ring, which is present in the eyes of extant saurospids, excluding crocodiles and snakes, and is variously preserved in fossil taxa. However, there have been only a few studies investigating the relationships between the size, the scleral ossicle ring, and soft structures of the eye. We investigated such relationships among the eye structures in extant Squamata, to establish the basis for inferring the size of the soft structures in the eye in fossil squamates. Three-dimensional morphological data on the eye and head region of 59 lizard species covering most major clades were collected using micro-computed tomography scanners. Strong correlations were found between the internal and external diameters of the scleral ossicle ring and soft structures. The tight correlations found here will allow reliable estimations of the sizes of soft structures and inferences on the visual performance and mode of life in fossil squamates, based on the diameters of their preserved scleral ossicle rings. Furthermore, the comparison of the allometric relationships between structures in squamates eyes with those in avian eyes suggest the possibility that the similarities of these structures closely reflect the mechanism of accommodation.

KEYWORDS

allometric relationships, scleral ossicle ring, squamates eyes

1 | INTRODUCTION

Visual performance is related to the mode of animal life, both in invertebrates and vertebrates (Land & Nilsson, 2002; Walls, 1942). Visual information is used for various purposes including detecting preys, avoiding predators, and finding and selecting mates (Cott, 1940; Loyau et al., 2005, 2007; Pettigrew et al., 1999). Eye structures vary in size and shape depending on the activity pattern related to light level, that is, diurnality or nocturnality, as well as underwater behaviors, in vertebrates (Land & Nilsson, 2002; Luria & Kinney, 1970). For example, the size of the cornea relative to the axial length (AL) of the eyeball and the shape of the pupil differ

between diurnal and nocturnal species among lizards (Hall, 2008a), birds (Hall & Ross, 2007; Malmström & Kröger, 2006), and mammals (Banks et al., 2015; Kirk, 2004). Diving behavior also has a large influence on eye structures such as the size and shape of the lens in various taxa (Land & Nilsson, 2002; Thewissen & Nummela, 2008). This is because light level is also affected by water depth and also because light refraction is different between air and water (Luria & Kinney, 1970; Warrant & Locket, 2004). Such relationships between eye morphology and lifestyle provide a solid basis for investigating the mode of life in fossil taxa, for which lifestyle cannot be observed directly (Motani et al., 1999; Schmitz & Motani, 2011).

The different activity patterns described above are reflected by modifications of the skeletal structures associated with the eye (e.g., Atkins & Franz-Odendaal, 2016; Caprette et al., 2004; Curtis & Miller, 1938; Fernández et al., 2005; Franz-Odendaal, 2008; Hall, 2008b; Hall et al., 2009; Kay & Cartmill, 1977; Kay & Kirk, 2000; Kirk, 2006; Pilgrim & Franz-Odendaal, 2009; Schmitz & Motani, 2010). For example, a characteristic shape of the orbit is known for diurnal mammals (Kirk, 2006). The size and/or ring of scleral ossicles, the skeletal structure embedded within the eyes in lizards and birds, also reflect activity patterns. The morphology of the scleral ossicle ring varies depending on animal lifestyles such as diurnality versus nocturnality, flying, and diving (Atkins & Franz-Odendaal, 2016; Curtis & Miller, 1938; Hall, 2008b, 2009; Martin & Brooke, 1991). The scleral ossicle ring is the only hard structure present within the eye that may be preserved in fossil saurospids (e.g., Dollo, 1889; Edinger, 1929; Marsh, 1880; Plisnier-Ladame & Coupatez, 1969). Thus, this structure potentially provides crucial information on the visual function in extinct species, especially if functionally relevant structures of the eye can be estimated based on its size preserved in fossils. The inferred visual function will then allow us to discuss the mode of life in extinct species from a hitherto rarely focused point of view. Previously, only a few activity patterns (e.g., diurnal or nocturnal activity) have been demonstrated to be correlated with the shape of eye structures. Schmitz (2009) showed that the sizes of hard tissue structures such as the scleral ossicle ring and the orbit are closely correlated with those of soft tissue structures such as the AL, lens diameter (LD), and maximum entrance pupil diameter (A) in avian eyes. Similar correlations between the hard and soft tissue structures were also shown in lepidosaurs by Hall (2009). However, the measurements of soft tissues analyzed in Hall (2009) were limited to external structures of an eye such as corneal diameter and AL, and did not include internal structures of an eye such as the A and LD. The visual function of the eye is constrained not only by external sizes but also by internal structures (Land, 1981). For example, light sensitivity, which is a measurement reflecting the ability of an eye detecting an object in the dark environments. It is commonly expressed as *f*-number, that is, the ratio between the A and the focal length (Land, 1981; Martin, 1982, 1983). An animal eye with a low *f*-number can see objects in darker and greater water depth than one with a high *f*-number because of its capability of collecting greater amount of light. Therefore, inferences on *f*-numbers in fossil taxa provide an important clue for exploring their visual functions in a quantitative way.

The aim of this study is to establish the relationships in squamate eyes between the sizes of soft tissue structures, that is, LD, A, AL, and eyeball diameter (ED), which are not preserved in fossils, and internal and external scleral ossicle ring diameters (INT and EXT). As fairly tight correlations have already been established between sizes of these structures in Aves (e.g., Schmitz, 2009), it is expected that similarly tight correlations exist in eyes in Squamata, considering the eye structures are similar between these two clades (Land & Nilsson, 2002). Such correlations will then serve as a basis for estimating visual functions in fossil squamate taxa and, in turn, their mode of life.

2 | MATERIALS AND METHODS

2.1 | Materials

Taxon sampling in this study covered most major clades in Squamata. Exceptions were Serpentes and Amphisbaenia, which were excluded from the present analysis, because the scleral ossicle ring is vestigial or absent in them. All examined specimens were obtained from either the Division of Amphibians and Reptiles, Department of Zoology, the Field Museum (FMNH) or iZoo. Specimens from the Field Museum had been preserved in 70% ethanol. In each specimen, the eyeball was removed from the orbit. All ocular muscles and fascia attached to the eyeball were then removed before measurement of structures. The individuals obtained from iZoo had been frozen after their death. The head was removed from the rest of the body and was initially fixed in 10% buffered formalin for 3 days before transferred to 70% ethanol. The specimens obtained from iZoo are housed at The University Museum, The University of Tokyo. A complete list of the specimen studies including collection numbers is given in Tables 1–7.

2.2 | CT scanning and measurement of eye structures

All specimens were micro-computed tomography (CT)-scanned using a Microfocus CT TXS 320-ACTIS (TESCO) at the National Museum of Nature and Science in Tokyo and/or Microfocus CT HMX 225-ACTIS + 3 (TESCO) at the Center for Advanced Marine Core Research, Kochi University in Kochi. Scans at the National Museum of Nature and Science were performed at 200 kV and 190 μA, with isotropic voxel resolutions of images varying from 0.033 to 0.040 mm. At the Center for advanced Marine Core Research, specimens were scanned at 30 kV and 100 μA, with isotropic voxel resolutions varying from 0.02 to 0.01 mm.

The following measurements were made on each specimen: postmortem A, LD, eyeball AL, and ED among soft tissue structures, as well as INT and EXT among hard tissue structures (Figure 1).

The measurement procedure was as follows. We measured the dimensions of the hard tissue structures on the ethanol-preserved specimens. CT images of the removed heads (specimens from iZoo)

TABLE 1 Dimensions of the INT and the LD

Super family	Family	Species	Collection no.	INT (mm)	LD (mm)
Gekkota	Carphodactylidae	*Nephrurus amyae*	UMUT RV33909	7.33	5.71
	Eublepharidae	*Eublepharis macularius*	UMUT RV33910	4.39	3.37
		Gonatodes ceciliae	FMNH 176870	2.10	1.50
	Sphaerodactylidae	*Teratoscincus scincus*	FMNH 200202	4.61	3.41
		Thecadactylus rapicauda	FMNH 40669	5.45	4.09
	Phyllodactylidae	*Tarentola boehmei*	FMNH 197520	4.71	3.08
	Gekkonidae	*Chondrodactylus turneri*	FMNH 78150	5.81	4.39
		Gekko gecko	UMUT RV33911	9.20	6.30
		Cyrtodactylus pubisulcus	FMNH 150593	4.66	3.13
Scincoidea	Scincidae	*Chalcides ocellatus*	FMNH 83659	1.92	2.11
		Eumeces schneideri	UMUT RV33394	2.66	3.04
		Tropidophorus brookei	FMNH 246315	3.48	3.09
		Eutropis multifasciata	FMNH 138491	3.78	3.06
Lacertoidea	Teiidae	*Aspidoscelis calidipes*	FMNH 109544	1.89	2.35
		Dicrodon guttulatum	FMNH 53849	3.27	2.93
		Cnemidophorus lemniscatus	FMNH 166998	2.53	2.52
		Ameiva festiva	FMNH 115441	3.70	2.99
		Teius teyou	FMNH 10864	3.24	2.85
	Gymnophthalmidae	*Gelanesaurus cochranae*	FMNH 23524	2.90	2.24
	Lacertidae	*Gallotia galloti*	FMNH 197399	2.49	2.80
		Eremias grammica	FMNH 83968	2.10	1.91
		Nucras ornatu	FMNH 22089	2.14	1.68
		Lacerta trilineata trilineata	FMNH 66689	3.48	2.73
Anguimorpha	Anguidae	*Barisia imbricata*	FMNH 71024	2.16	1.85
	Xenosauridae	*Xenosaurus grandis*	FMNH 123700	3.44	3.13
	Varanidae	*Varanus albigularis*	UMUT RV33395	4.38	4.86
Iguania	Chamaeleonidae	*Trioceros melleri*	UMUT RV33912	3.62	3.89
	Agamidae	*Physignathus cocincinus*	UMUT RV33393	3.51	3.69
		Bronchocela cristatella	FMNH 184532	3.81	3.79
		Paralaudakia caucasia	FMNH 171155	3.06	3.61
		Trapelus mutabilis	UMUT RV33913	2.34	2.86
	Iguanidae	*Ctenosaura similis*	FMNH 5184	4.44	4.10
		Ctenosaura quinquecarinata	FMNH 176685	2.62	2.89
	Corytophanidae	*Basiliscus vittatus*	FMNH 34599	4.42	4.17
	Crotaphytidae	*Crotaphytus collaris*	UMUT RV33914	2.89	3.43
	Tropiduridae	*Stenocercus chrysopygus*	FMNH 81426	2.15	2.07
		Microlophus peruvianus	FMNH 68559	2.67	2.96
		Tropidurus habeli	FMNH 37249	2.23	2.59
	Liolaemidae	*Liolaemus tenuis*	FMNH 209026	1.75	1.98

TABLE 1 (Continued)

Super family	Family	Species	Collection no.	INT (mm)	LD (mm)
		Liolaemus andinus	FMNH 39434	1.71	1.96
	Phrynosomatidae	*Uma scoparia*	FMNH 1203	2.17	2.32
		Cophosaurus texanus	FMNH 47310	1.76	2.09
		Petrosaurus thalassinus	FMNH 223967	2.76	2.85
		Phrynosoma platyhinos	FMNH 283964	2.23	2.51
		Sceloporus olivaceus	FMNH 27195	2.42	2.63
	Dactyloidae	*Anolis carolinensis*	UMUT RV33915	1.71	2.29
		Anolis bimaculatus	FMNH 11894	2.35	3.02
		Anolis biporcatus	FMNH 49207	3.11	4.00

Abbreviations: INT, internal scleral ossicle ring diameter; LD, lens diameter.

or eyeballs (specimens from FMNH) were used to measure INT and EXT on the transverse sectional images produced by Osirix v.7.0.3 (Figure 2a).

We then measured exterior dimensions such as A, AL, and ED (Figure 2b,c) on ethanol-preserved specimens using ImageJ (64 bit; Schneider et al., 2012) on photo images taken by a digital camera-equipped stereomicroscope (Nikon SMZ1000). Before photos were taken, each eyeball was re-inflated with 70% ethanol using a small gauge injection needle until the eye regained a globose shape and could not be inflated any further following published procedures (Hall, 2008a, 2009; Kirk, 2004; Schmitz, 2009). To measure the soft tissue structurers inside of the eyeball, 70% ethanol-preserved specimens were stained with a 1% Lugol's solution (iodine potassium iodide) for a period between 1 day (eyeball specimens) to a few weeks (head specimens), depending on the size (diffusible iodine-based contrast-enhanced CT or diceCT; Gignac & Kley, 2014). These stained specimens were CT-scanned again for measuring LD on contrast images using Osirix 7.0.3. All dimensions of structures were measured for three times and the mean values were used for comparisons.

Whereas the staining method using iodine potassium iodide has been demonstrated effective in anatomical visualization, previous studies also point to the problem of deformation of specimens such as shrinkage caused by immersion in an iodine potassium iodide solution (Pauwels et al., 2013; Vickerton et al., 2013; Wong et al., 2013). In this study, the size change in each structure in the eyes during staining for contrast-enhanced CT scanning was investigated. Eyes were dissected out from five specimens of lizards belonging to five genera (*Hemidactylus platyurus*, *Gekko vittatus*, *Iguana iguana*, *Agama agama*, and *Varanus exanthematicus*), ranging from 2.3 to 310 g in body mass. These five lizard specimens were euthanized by decapitating them after whole-body cooling above or near the freezing point. Immediately after each eyeball was removed from the orbit, the baseline volume was measured. The sampled eyes were then fixed with 10% neutral buffered formalin and were subsequently removed into 70% ethanol before being stained in a 1% iodine potassium iodide solution. The LD was measured based on photographs of specimens taken using a stereomicroscope. All procedures were performed in accordance with the protocols approved by the University of Tokyo Animal Care Committee (permission number 15-4). As a result, iodine staining caused the shrinkage to 93%, 87%, 88%, 86%, and 86% of the original LD in *Agama*, *Varanus*, *Gekko*, *Hemidactylus*, and *Iguana*, respectively. This result indicates that it is necessary to restore the LDs to the original, prestained values in specimens analyzed using contrast-enhanced CT scanning. Based on these observations, the LDs measured on dice-CT images were restored in the following ways. First, for the five species of which degree of shrinkage was directly examined herein, the values measured before iodine potassium iodide staining were used. Second, the measurements taken on dice-CT images for other species were assumed to have shrunk with the average ratio of those five species (*Agama*, *Varanus*, *Gekko*, *Hemidactylus*, and *Iguana*). That is, the LDs before iodine potassium iodide staining were restored by multiplying the measurements by the inverse of the average ratio, that is, 1.34.

2.3 | Analyses of correlations between the soft and hard tissue structures

We a statistically analyzed correlations between the following pairs of measurements:

1. The correlation between INT and LD was analyzed for 48 species belonging to 45 genera of squamates including the clades Eublepharidae, Sphaerodactylidae, Phyllodactylidae, Gekkonidae, Carphodactylidae, Scincidae, Lacertidae, Gymnophthalmidae, Teiidae, Xenosauridae, Varanidae, Chamaeleonidae, Agamidae, Iguanidae, Corytophanidae, Crotaphytidae, Tropiduridae, Liolaemidae, Phrynosomatidae, and Dactyloidae (Table 1).
2. The correlation between INT and A was analyzed for 38 species belonging to 35 genera included in the clades

TABLE 2 Dimensions of the INT and the A

Super family	Family	Species	Collection no.	INT (mm)	A (mm)
Gekkota	Sphaerodactylidae	*Gonatodes ceciliae*	FMNH 176870	2.10	0.81
Scincoidea	Scincidae	*Lepidophyma smithii*	FMNH 123947	2.44	1.63
		Chalcides ocellatus	FMNH 83659	1.92	1.08
		Tropidophorus brookei	FMNH 246315	3.48	1.50
		Eutropis multifasciata	FMNH 138491	3.78	1.86
		Tiliqua rugosa	FMNH 212319	3.70	1.41
Lacertoidea	Lacertidae	*Lacerta trilineata trilineata*	FMNH 66689	3.48	1.86
		Eremias grammica	FMNH 83968	2.10	1.01
		Nucras ornata	FMNH 22089	2.14	1.11
	Gymnophthalmidae	*Gelanesaurus cochranae*	FMNH 23524	2.90	1.67
		Echinosaura horrida	FMNH 177474	2.51	1.13
	Teiidae	*Teius teyou*	FMNH 10864	3.24	1.91
		Cnemidophorus lemniscatus	FMNH 166998	2.53	1.31
		Holcosus festivus	FMNH 115441	3.70	2.21
		Dicrodon guttulatum	FMNH 53849	3.27	2.03
		Aspidoscelis calidipes	FMNH 109544	1.89	1.48
Anguimorpha	Xenosauridae	*Xenosaurus grandis*	FMNH 208059	2.93	1.43
	Anguidae	*Barisia imbricata*	FMNH 71024	2.16	1.12
		Mesaspis gadovii	FMNH 38522	1.87	0.90
Iguania	Agamidae	*Leiolepis rubritaeniata*	FMNH 181058	3.55	1.93
		Paralaudakia caucasia	FMNH 171155	3.06	1.09
		Calotes mystaceus	FMNH 180449	2.46	1.77
		Bronchocela cristatella	FMNH 184532	3.81	1.99
	Iguanidae	*Ctenosaura similis*	FMNH 5184	4.44	2.19
		Ctenosaura quinquecarinata	FMNH 176685	2.63	1.29
	Corytophanidae	*Basiliscus vittatus*	FMNH 34601	4.07	1.67
		Basiliscus basiliscus	FMNH 165546	3.45	2.02
	Tropiduridae	*Microlophus peruvianus*	FMNH 68559	2.67	1.11
		Stenocercus chrysopygus	FMNH 81426	2.15	0.89
	Liolaemidae	*Liolaemus andinus*	FMNH 39434	1.71	1.05
	Phrynosomatidae	*Petrosaurus thalassinus*	FMNH 223967	2.67	1.31
		Uta stansburiana	FMNH 130358	1.63	0.87
		Sceloporus olivaceus	FMNH 27195	2.42	1.30
		Uma scoparia	FMNH 1203	2.17	1.05
		Cophosaurus texanus	FMNH 47310	1.76	0.88
		Phrynosoma platyrhinos	FMNH 283964	2.23	1.06
	Dactyloidae	*Anolis bimaculatus*	FMNH 11894	2.35	1.44
		Anolis biporcatus	FMNH 49207	3.11	1.73

Abbreviations: A, pupil diameter; INT, internal scleral ossicle ring diameter.

TABLE 3 Dimensions of the EXT of the scleral ossicle ring and the AL

Super family	Family	Species	Collection no.	EXT (mm)	AL (mm)
Gekkota	Phyllodactylidae	*Aeluroscalabotes felinus*	FMNH 146061	7.43	7.24
		Teratoscincus scincus	FMNH 200202	6.13	6.51
		Thecadactylus rapicauda	FMNH 40669	6.62	6.05
		Homonota darwinii	FMNH 133652	3.26	3.47
	Gekkonidae	*Chondrodactylus turneri*	FMNH 78150	7.07	7.00
		Cyrtodactylus pubisulcus	FMNH 150593	5.32	5.36
		Gekko lionotum	FMNH 181830	6.90	6.53
Scincoidea	Scincidae	*Tropidophorus brookei*	FMNH 246315	6.69	5.88
		Eutropis multifasciata	FMNH 138491	7.29	6.04
		Chalcides ocellatus	FMNH 83659	4.35	3.87
	Xantusiidae	*Lepidophyma smithii*	FMNH 123947	4.06	3.74
Lacertoidea	Gymnophthalmidae	*Echinosaura horrida*	FMNH 177474	4.78	4.13
		Gelanesaurus cochranae	FMNH 23524	5.46	4.54
	Teiidae	*Teius teyou*	FMNH 10864	7.63	6.05
		Dicrodon guttulatum	FMNH 53849	7.87	6.41
	Lacertidae	*Gallotia galloti*	FMNH 197399	5.97	4.87
		Eremias grammica	FMNH 83968	5.84	5.06
Anguimorpha	Xenosauridae	*Xenosaurus grandis*	FMNH 208059	5.76	5.05
Iguania	Agamidae	*Calotes mystaceus*	FMNH 180449	6.31	7.13
	Iguanidae	*Ctenosaura similis*	FMNH 5184	10.46	9.67
		Ctenosaura quinquecarinata	FMNH 176685	5.95	6.03
	Corytophanidae	*Basiliscus vittatus*	FMNH 34599	8.23	7.76
		Basiliscus basiliscus	FMNH 165546	6.96	6.43
	Corytophanidae	*Stenocercus chrysopygus*	FMNH 81426	5.38	4.73
		Microlophus habelii	FMNH 37249	5.13	5.18
		Microlophus peruvianus	FMNH 68559	6.49	5.98
	Liolaemidae	*Liolaemus andinus*	FMNH 39434	3.88	4.19
	Dactyloidae	*Anolis bimaculatus*	FMNH 11894	5.25	5.17
		Anolis biporcatus	FMNH 49207	6.81	6.12
	Phrynosomatidae	*Phrynosoma platyrhinos*	FMNH 283964	8.20	6.16
		Uma scoparia	FMNH 1203	5.11	6.02
		Sceloporus olivaceus	FMNH 27195	6.44	5.81
		Uta stansburiana	FMNH 130358	4.15	3.88
		Petrosaurus thalassinus	FMNH 223967	6.87	6.27

Abbreviations: EXT, external diameter; AL, axial length.

Sphaerodactylidae, Scincidae, Lacertidae, Gymnophthalmidae, Teiidae, Xenosauridae, Anguidae, Agamidae, Iguanidae, Corytophanidae, Tropiduridae, Liolaemidae, Phrynosomatidae, and Dactyloidae (Table 2).

3. The correlation between EXT and AL was analyzed for 34 species belonging to 31 genera included in the clades Phyllodactylidae, Gekkonidae, Scincidae, Xantusiidae, Gymnophthalmidae, Teiidae, Lacertidae, Xenosauridae, Agamidae, Iguanidae, Corytophanidae,

TABLE 4 Dimensions of the EXT of the scleral ossicle ring and the ED

Super family	Family	Species	Collection no.	EXT (mm)	ED (mm)
Gekkota	Phyllodactylidae	*Aeluroscalabotes felinus*	FMNH 146061	7.43	7.69
		Teratoscincus scincus	FMNH 200202	6.13	6.88
		Thecadactylus rapicauda	FMNH 40669	6.62	7.07
		Homonota darwinii	FMNH 133652	3.26	3.47
	Gekkonidae	*Chondrodactylus turneri*	FMNH 78150	7.07	7.37
		Cyrtodactylus pubisulcus	FMNH 150593	5.32	5.62
		Gekko lionotum	FMNH 181830	6.90	7.47
Scincoidea	Scincidae	*Tropidophorus brookei*	FMNH 246315	6.69	6.93
		Eutropis multifasciata	FMNH 138491	7.29	7.12
		Chalcides ocellatus	FMNH 83659	4.35	4.42
	Xantusiidae	*Lepidophyma smithii*	FMNH 123947	4.06	4.17
Lacertoidea	Gymnophthalmidae	*Echinosaura horrida*	FMNH 177474	4.78	4.78
		Gelanesaurus cochranae	FMNH 23524	5.46	5.45
	Teiidae	*Teius teyou*	FMNH 10864	7.63	7.65
		Dicrodon guttulatum	FMNH 53849	7.87	7.93
	Lacertidae	*Gallotia galloti*	FMNH 197399	5.97	6.06
		Eremias grammica	FMNH 83968	5.84	6.02
		Nucras ornatu	FMNH 22089	4.51	4.64
Anguimorpha	Xenosauridae	*Xenosaurus grandis*	FMNH 208059	5.76	5.88
Iguania	Agamidae	*Calotes mystaceus*	FMNH 180449	6.31	8.65
		Bronchocela cristatella	FMNH 184532	7.80	8.12
	Iguanidae	*Ctenosaura similis*	FMNH 5184	10.46	11.74
		Ctenosaura quinquecarinata	FMNH 176685	5.95	7.43
	Corytophanidae	*Basiliscus vittatus*	FMNH 34599	8.23	9.29
		Basiliscus basiliscus	FMNH 165546	6.96	8.11
		Stenocercus chrysopygus	FMNH 81426	5.38	5.81
		Microlophus habelii	FMNH 37249	5.13	6.08
		Microlophus peruvianus	FMNH 68559	6.49	7.19
	Liolaemidae	*Liolaemus andinus*	FMNH 39434	3.88	4.85
	Dactyloidae	*Anolis bimaculatus*	FMNH 11894	5.25	6.20
		Anolis biporcatus	FMNH 49207	6.81	7.25
	Phrynosomatidae	*Phrynosoma platyrhinos*	FMNH 283964	8.20	8.09
		Uma scoparia	FMNH 1203	5.11	7.49
		Sceloporus olivaceus	FMNH 27195	6.44	7.09
		Uta stansburiana	FMNH 130358	4.15	4.64
		Petrosaurus thalassinus	FMNH 223967	6.87	7.74

Abbreviations: EXT, external diameter; ED, eyeball diameter.

TABLE 5 Dimensions of the LD and A

Super family	Family	Species	Collection no.	LD (mm)	A (mm)
Gekkota	Eublepharidae	*Gonatodes ceciliae*	FMNH 176870	1.50	0.81
Scincoidea	Scincidae	*Chalcides ocellatus*	FMNH 83659	2.11	1.08
		Tropidophorus brookei	FMNH 246315	3.09	1.50
		Eutropis multifasciata	FMNH 138491	3.06	1.86
Lacertoidea	Teiidae	*Aspidoscelis calidipes*	FMNH 109544	2.35	1.48
		Dicrodon guttulatum	FMNH 53849	2.93	2.03
		Cnemidophorus lemniscatus	FMNH 166998	2.52	1.31
		Ameiva festiva	FMNH 115441	2.99	2.21
		Teius teyou	FMNH 10864	2.85	1.91
	Gymnophthalmidae	*Gelanesaurus cochranae*	FMNH 23524	2.24	1.67
	Lacertidae	*Eremias grammica*	FMNH 83968	1.91	1.01
		Nucras ornatu	FMNH 22089	1.68	1.11
		Lacerta trilineata trilineata	FMNH 66689	2.73	1.86
Anguimorpha	Anguidae	*Barisia imbricata*	FMNH 71024	1.85	1.12
	Xenosauridae	*Xenosaurus grandis*	FMNH 208059	2.43	1.43
Iguania	Agamidae	*Bronchocela cristatella*	FMNH 184532	3.79	1.99
		Paralaudakia caucasia	FMNH 171155	3.61	1.06
	Iguanidae	*Ctenosaura similis*	FMNH 5184	4.10	2.19
		Ctenosaura quinquecarinata	FMNH 176685	2.89	1.29
	Corytophanidae	*Basiliscus vittatus*	FMNH 34599	4.17	2.15
	Tropiduridae	*Stenocercus chrysopygus*	FMNH 81426	2.07	0.98
		Microlophus peruvianus	FMNH 68559	2.96	1.11
	Liolaemidae	*Liolaemus andinus*	FMNH 39434	1.96	1.05
	Phrynosomatidae	*Uma scoparia*	FMNH 1203	2.32	1.05
		Cophosaurus texanus	FMNH 47310	2.09	0.88
		Petrosaurus thalassinus	FMNH 223967	2.85	1.31
		Phrynosoma platyhinos	FMNH 283964	2.51	1.06
		Sceloporus olivaceus	FMNH 27195	2.63	1.30
	Dactyloidae	*Anolis bimaculatus*	FMNH 11894	3.02	1.44
		Anolis biporcatus	FMNH 49207	4.00	1.73

Abbreviations: A, pupil diameter; LD, lens diameter.

Tropiduridae, Liolaemidae, Dactyloidae, and Phrynosomatidae (Table 3).

4. The correlation between EXT and ED was analyzed for 36 species belonging to 32 genera included in the clades Phyllodactylidae, Gekkonidae, Scincidae, Xantusiidae, Gymnophthalmidae, Teiidae, Lacertidae, Xenosauridae, Agamidae, Iguanidae, Corytophanidae, Liolaemidae, Dactyloidae, and Phrynosomatidae (Table 4).
5. The correlation between LD and A was analyzed for 30 species belonging to 28 genera included in the clades Eublepharidae, Scincidae, Gymnophthalmidae, Teiidae, Lacertidae, Xenosauridae, Anguidae, Agamidae, Iguanidae, Tropiduridae, Corytophanidae, Liolaemidae, Dactyloidae, and Phrynosomatidae (Table 5).
6. The correlation between ED and AL was analyzed for 34 species belonging to 30 genera included in the clades Phyllodactylidae, Gekkonidae, Scincidae, Xantusiidae, Gymnophthalmidae, Teiidae, Lacertidae, Xenosauridae, Agamidae, Iguanidae, Corytophanidae, Liolaemidae, Dactyloidae, and Phrynosomatidae (Table 6).

For these correlations, we used linear regression methods, ordinary least square (OLS) regression and reduced major axis

TABLE 6 Dimensions of the ED and the AL in the examined squamates

Super family	Family	Species	Collection no.	ED (mm)	AL (mm)
Gekkota	Phyllodactylidae	*Aeluroscalabotes felinus*	FMNH 146061	7.56	7.24
		Teratoscincus scincus	FMNH 200202	6.88	6.51
		Thecadactylus rapicauda	FMNH 40669	7.07	6.05
		Homonota darwinii	FMNH 133652	3.47	3.47
	Gekkonidae	*Chondrodactylus turneri*	FMNH 78150	7.37	7.00
		Cyrtodactylus pubisulcus	FMNH 150593	5.62	5.36
		Gekko lionotum	FMNH 181830	7.47	6.53
Scincoidea	Scincidae	*Tropidophorus brookei*	FMNH 246315	6.93	5.88
		Eutropis multifasciata	FMNH 138491	7.12	6.04
		Chalcides ocellatus	FMNH 83659	4.42	3.87
	Xantusiidae	*Lepidophyma smithii*	FMNH 123947	4.17	3.74
Lacertoidea	Gymnophthalmidae	*Echinosaura horrida*	FMNH 177474	4.78	4.13
		Gelanesaurus cochranae	FMNH 23524	5.45	4.54
	Teiidae	*Teius teyou*	FMNH 10864	7.65	6.05
		Dicrodon guttulatum	FMNH 53849	7.93	6.41
	Lacertidae	*Gallotia galloti*	FMNH 197399	6.06	4.87
		Eremias grammica	FMNH 83968	6.02	5.06
Anguimorpha	Xenosauridae	*Xenosaurus grandis*	FMNH 208059	5.88	5.05
Iguania	Agamidae	*Calotes mystaceus*	FMNH 180449	8.65	7.13
	Iguanidae	*Ctenosaura similis*	FMNH 5184	11.74	9.67
		Ctenosaura quinquecarinata	FMNH 176685	7.43	6.03
	Corytophanidae	*Basiliscus vittatus*	FMNH 34599	9.29	7.76
		Basiliscus basiliscus	FMNH 165546	8.11	6.43
		Stenocercus chrysopygus	FMNH 81426	5.81	4.73
		Microlophus habelii	FMNH 37249	6.08	5.18
		Microlophus peruvianus	FMNH 68559	7.19	5.98
	Liolaemidae	*Liolaemus andinus*	FMNH 39434	4.85	4.19
	Dactyloidae	*Anolis bimaculatus*	FMNH 11894	6.20	5.17
		Anolis biporcatus	FMNH 49207	7.25	6.12
	Phrynosomatidae	*Phrynosoma platyrhinos*	FMNH 283964	8.09	6.16
		Uma scoparia	FMNH 1203	7.49	6.02
		Sceloporus olivaceus	FMNH 27195	7.09	5.81
		Uta stansburiana	FMNH 130358	4.64	3.88
		Petrosaurus thalassinus	FMNH 223967	7.74	6.27

Abbreviations: AL, axial length; ED, eyeball diameter.

(RMA) regression. The allometric relationship of the variable *Y* to the variable *X* is expressed as the equation

$$Y = bX^a$$

where *a* is the allometry coefficient, that is, the slope of the allometric line. When a equals 1.0, the variable *Y* scales isometrically with the variable *X*, that is, *Y* increases at the same rate as *X* (Gould, 1966; Huxley, 1932). When $a > 1$, *Y* increases at a greater rate than does *X*

TABLE 7 Summary of the results on correlation analyses between the sizes of hard and soft tissue parameters in squamates

			OLS		RMA		PGLS		
Hard-tissue variable	**Soft-tissue variable**	r^2	**Slope (95% CI)**	***p***	**Slope (95% CI)**	***p***	r^2	**Slope**	**λ**
INT	LD	.75	0.67 (0.55–0.78)	<.001	0.77 (0.67–0.90)	<.001	.76	0.74	0.57
INT	A	.66	0.87 (0.66–1.08)	.23	1. 07 (0.88–1.31)	.47	.68	0.85	0.39
EXT	AL	.83	0.85 (0.71–0.99)	.03	0.93 (0.80–1.08)	.34	.83	0.86	0.51
EXT	ED	.89	0.96 (0.84–1.07)	.45	1.01 (0.90–1.14)	.80	.89	0.91	0.47
Soft-tissue variable	**Soft-tissue variable**								
LD	A	.51	0.81 (0.50–1.11)	.21	1.13 (0.86–1.47)	.37	.71	1.03	0.87
ED	AL	.94	0.89 (0.81–0.96)	.006	0.91 (0.84–0.99)	.03	.97	0.91	0.81

Abbreviations: A, pupil diameter; AL, axial length; CI, confidence intervals; ED, eyeball diameter; EXT, external scleral ossicle ring diameter; INT, internal scleral ossicle ring diameter; LD, lens diameter; OLS, ordinary least square; PGLS, phylogenetic generalized least squares; RMA, reduced major axis.

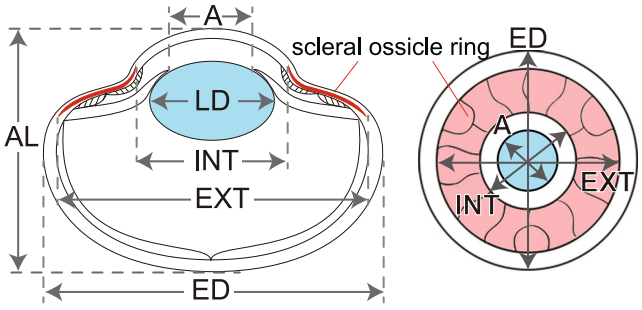

FIGURE 1 Semi-diagrammatic cross-section and frontal view of a lizard eyeball with anatomical measurements. A, pupil diameter; AL, eyeball axial length; ED, eyeball diameter; EXT, external scleral ossicle ring diameter; INT, internal scleral ossicle ring diameter; LD, equatorial lens diameter.

(positive allometry), whereas *Y* increases at a lower rate than does *X* (negative allometry) when $a < 1$. By log 10-transforming the equation, it becomes:

$$\log Y = \log b + a \log X$$

Thus, log *Y* and log *X* show a linear relationship with the slope *a*. In such a plot, a statistically significant difference between slope 1.0 and the estimated slope rejects the hypothesis of isometry between *X* and *Y*. Accordingly, for analyses of correlations among the variables mentioned above, we tested for a significant difference of the value of this slope from 1 with *p* taken from the F-distribution.

The aim of this study is to develop a method for estimating the sizes of soft tissue structures of the eye based on measurements of the scleral ossicle ring using the allometric equation explained above. The confidence interval (CI) is usually used as the parameter of accuracy of the estimation of the true regression (Heskes, 1996). That is, the 95% CI describes the range of the values that encompass the expected mean of *Y* that contains 95% of the sample means (Sokal & Rohlf, 1995). In contrast, the prediction interval (PI) is interpreted as the accuracy for our estimation with respect to the observed target value (Heskes, 1996). Thus, 95% PI

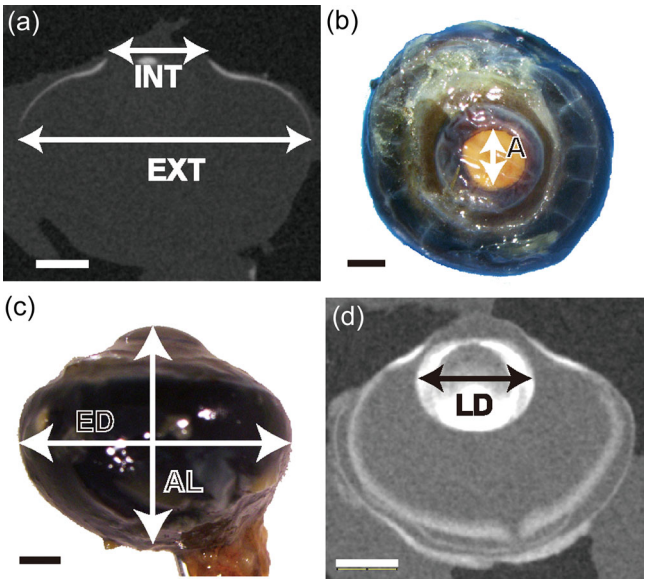

FIGURE 2 Measurements of eye structures. (a) Cross-sectional computed tomography (CT) image of a fixed eyeball specimen (FMNH 83968 *Eremias grammica*) for measurement of the internal and external diameter of the sclerotic ring (INT and EXT, respectively). (b) External view of the eyeball (FMNH 11894 *Anolis bimaculatus*) for measurement of pupil diameter (A). (c) Lateral view of an eyeball (FMNH 27195 *Sceloporus olivaceus*) for measurement of the eyeball axial length (AL) and eyeball diameter (ED). (d) Cross-sectional CT image of a specimen (FMNH 39434 *Liolaemus andinus*) stained with a 1% Lugol's solution for measurement of the equatorial lens diameter (LD). Scale bars = 1 mm.

describes the range of the values that encompass the expected mean of *Y* with 95% probability to contain the true mean adjusted for the new sample size (Sokal & Rohlf, 1995). It should be noted that PI is usually much wider than CI, but PI is of more practical use than CI in predictions that use a single observed target value (Heskes, 1996). Although we calculated CIs to assess the accuracy of the slope of allometric line, PIs were also used for estimation of eyeball soft-tissue dimension based on a certain value of a scleral ossicle ring.

Interspecific data are not considered phylogenetically independent, because closely related species are more likely to exhibit similar trait values. For this reason, we also used the phylogenetic generalized least squares (PGLS) regression model with Pagel's λ to remove the phylogenetic influence from the data for analyses of correlations. The parameter λ indicates the degree of the phylogenetic influence and ranges from 0 to 1. Higher λ values indicate stronger similarities between closely related taxa. Pagel's λ models are mathematically equivalent to the OLS regression analysis (i.e., with no phylogenetic correction) when λ = 0, whereas the presence of a strong phylogenetic signal consistent with gradual evolution via a Brownian motion model is suggested when λ = 1 (Freckleton et al., 2002; Harvey & Pagel, 1991; Pagel, 1999). The parameter λ for the relationship between each pair of hard and soft tissue structures was estimated with a variance–covariance matrix describing the phylogenetic relationship of species. For calculation of PGLS regression, a phylogenetic tree with information of branch lengths was produced using Mesquito v. 3.51 (Maddison & Maddison, 2018) based on Zheng and Wiens (2016). The time-calibrated phylogenetic trees for PGLS analysis are included in supplementary online material Supporting Information: Figures S1–S6. All calculations for the regression analyses (OLS and RMA) and PGLS regressions were carried out on log-transformed measurement values in R v. 3.4.0 (Harmon et al., 2008; Legendre, 2011; Orme et al., 2013; Paradis et al., 2004; Pinheiro et al., 2017; Revell, 2012; Warton et al., 2012).

3 | RESULTS

All correlations between the sizes related to the scleral ossicle ring and the relevant soft tissue structures were statistically significant (Table 7 and Figure 3). These linear regressions met assumptions of independence, homoscedasticity and normality in residuals (Supporting Information: Tables S1–S6). A strong correlation (R^2 = .75) was present between the INT and the LD. LD showed a significant negative allometry relative to INT in both OLS and RMA analyses (OLS slope = 0.67, OLS intercept = 0.20, CI = 0.55–0.78, p_{OLS} < 0.001; RMA slope = 0.77, RMA intercept = 0.15, CI = 0.67–0.90, p_{RMA} < 0.001). Thus, for example, an INT of 10 mm would predict an LD of 7.41 mm (PI: 5.61–9.55). As for the PGLS analysis, the dependent variable exhibited a phylogenetic signal (λ) of 0.57, which is significantly >0.0 (p = .002) and significantly <1.0 (p < .001). When the effect of phylogeny was removed from the data, the allometric slope and intercept were 0.74 and 0.15, respectively, and the strong correlation between INT and LD remained as shown by a coefficient of determination R^2 = .76 (Figure 4a).

Internal ossicle ring diameter also had a high coefficient of determination (R^2 = .66) with the A. The values of the slopes did not differ from 1.0 in either OLS or RMA, suggesting that A scaled isometrically with INT (OLS slope = 0.87, OLS intercept = −0.23, CI = 0.66–1.08, p_{OLS} = 0.23; RMA slope = 1.07, RMA intercept = −0.32, CI = 0.88–1.31, p_{RMA} = 0.47). Accordingly, an INT of 10 mm, for example, would predict a A of 4.37 mm (PI: 2.69–7.08). As for the PGLS analysis, the dependent variable exhibited a phylogenetic signal (λ) of 0.39, which is marginally >0.0 (p = .27) and significantly <1.0 (p = .006). When the effect of phylogeny was removed from the data, the allometric slope and intercept were 0.85 and −0.23, and the strong correlation between INT and A remained with a coefficient of determination R^2 = .68 (Figure 4b).

The correlation between the EXT and AL was also strong (R^2 = .83). AL scaled with significant negative allometry to EXT in OLS (OLS slope = 0.85, OLS intercept = 0.08, CI= 0.71–0.99, p_{OLS} = 0.03), whereas significant isometrical relation was shown in RMA (RMA slope = 0.93, RMA intercept = 0.02, CI= 0.80–1.08, p_{RMA} = 0.34). Thus, an EXT of 10 mm would predict an AL of 8.51 mm (PI: 6.21–11.75). As for the PGLS analysis, the dependent variable exhibited a phylogenetic signal (λ) of 0.51, which is significantly >0.0 (p = .04) and significantly <1.0 (p = .004). When the effect of phylogeny was removed from the data, the allometric slope and intercept were 0.83 and 0.09, and the strong correlation between EXT and AL remained with a coefficient of determination R^2 = .86 (Figure 4c).

A strong correlation (R^2 = .89) was present between EXT and the ED. ED scaled isometrically with EXT, both in OLS and RMA (OLS slope = 0.96, OLS intercept = 0.07, CI= 0.84–1.07, p_{OLS} = 0.45, RMA slope = 1.01, RMA intercept = 0.03, CI = 0.90–1.14, p_{RMA} = 0.80). Thus, an EXT of 10 mm predicts an ED of 10.71 mm (PI: 8.13–13.80). As for the PGLS analysis, the dependent variable exhibited a phylogenetic signal (λ) of 0.47, which is significantly >0.0 (p = .01) and significantly <1.0 (p = .006). The allometric slope and intercept were 0.91 and 0.09, and the strong correlation between EXT and ED remained with a coefficient of determination R^2 = .89 when the effect of phylogeny was removed from the data (Figure 4d).

Strong correlations were also present between soft tissue structures, for example, between LD and A (R^2 = .51). Pupil diameter (A) scaled isometrically with LD both in OLS and RMA (OLS slope = 0.81, OLS intercept = −0.25, CI = 0.50–1.11, p_{OLS} = 0.21, RMA slope = 1.13, RMA intercept = −0.40, CI = 0.86–1.47, p_{RMA} = 0.37). Thus, an LD of 10 mm would predict a maximum entrance A of 3.63 mm (PI: 1.78–7.24). As for the PGLS analysis, the dependent variable exhibited the strongest phylogenetic signal among the examined correlations (λ = 0.87), which is significantly >0.0 (p < .001) and marginally <1.0 (p = .46). The allometric slope and intercept were 1.03 and −0.33, and the strong correlation between LD and A remained with a coefficient of determination R^2 = .71 when the effect of phylogeny was removed from the data (Figure 4e).

The correlation between ED and AL was the strongest (R^2 = .94) among the examined correlations. AL scaled with significant negative allometry to ED both in OLS and RMA (OLS slope = 0.89, OLS intercept = 0.02, CI = 0.81–0.96, p_{OLS} = 0.006, RMA slope = 0.91, RMA intercept = −0.0005, CI = 0.84–0.99,

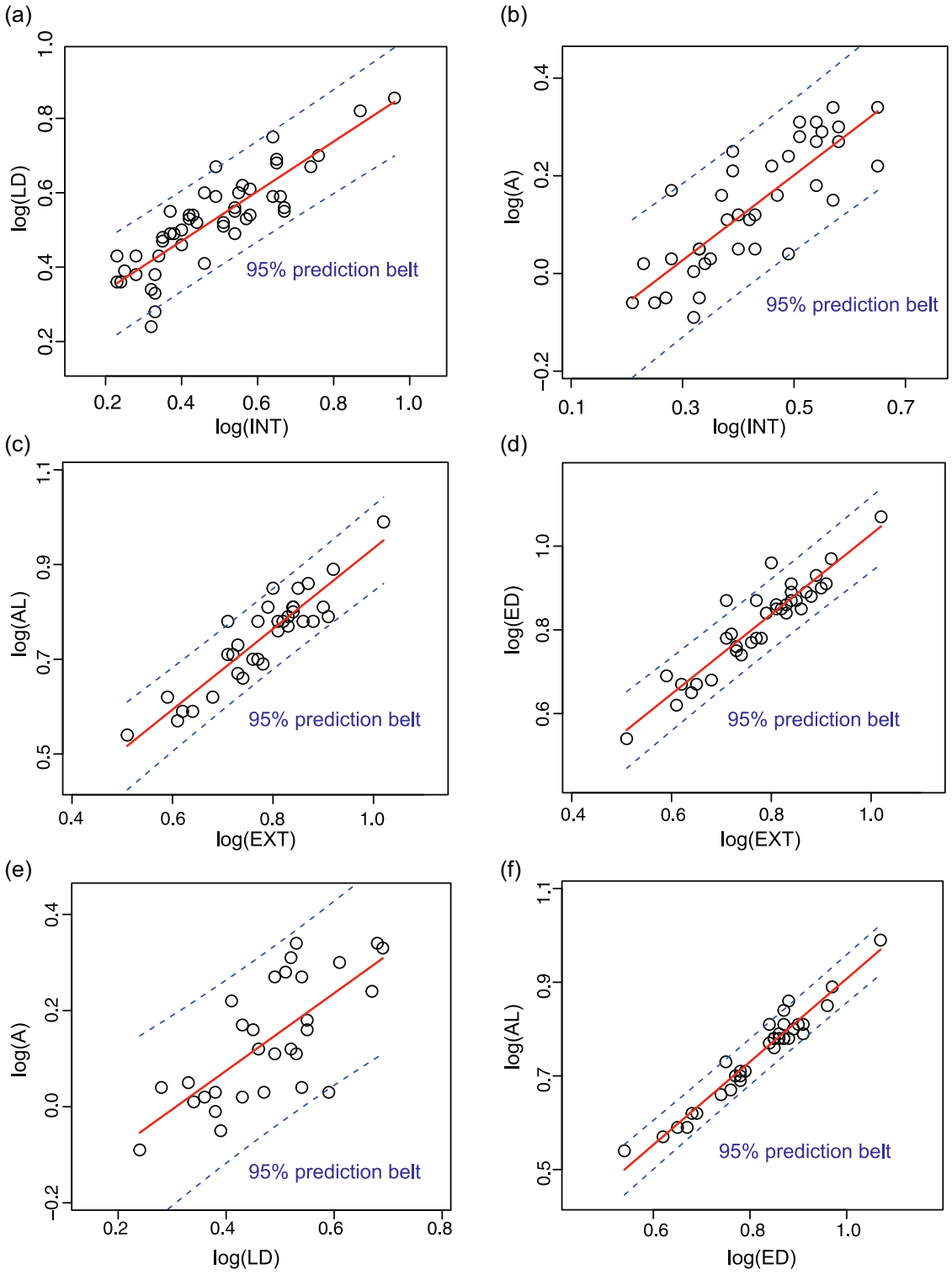

FIGURE 3 Relationship between soft and hard tissue variables of the eye. (a) Lens diameter (LD) and internal scleral ossicle ring diameter (INT). (b) Pupil diameter (A) and INT. (c) Axial length (AL) and external scleral ossicle ring diameter (EXT). (d) Eyeball diameter (ED) and EXT. (e) A and LD. (f) AL and ED. Regression statistics are based on OLS. All data had been log-transformed before analyses.

p_{RMA} = 0.03). An ED of 10 mm would predict an AL of 8.12 mm (PI: 6.76–9.55). As for the PGLS analysis, the dependent variable exhibited a phylogenetic signal (λ) of 0.81, which is significantly >0.0 (p < .001) and significantly <1.0 (p = .02). The allometric slope and intercept were 0.91 and 0.003, and the strong correlation between ED and AL remained with a coefficient of determination R^2 = .97 when the effect of phylogeny was removed from the data (Figure 4f).

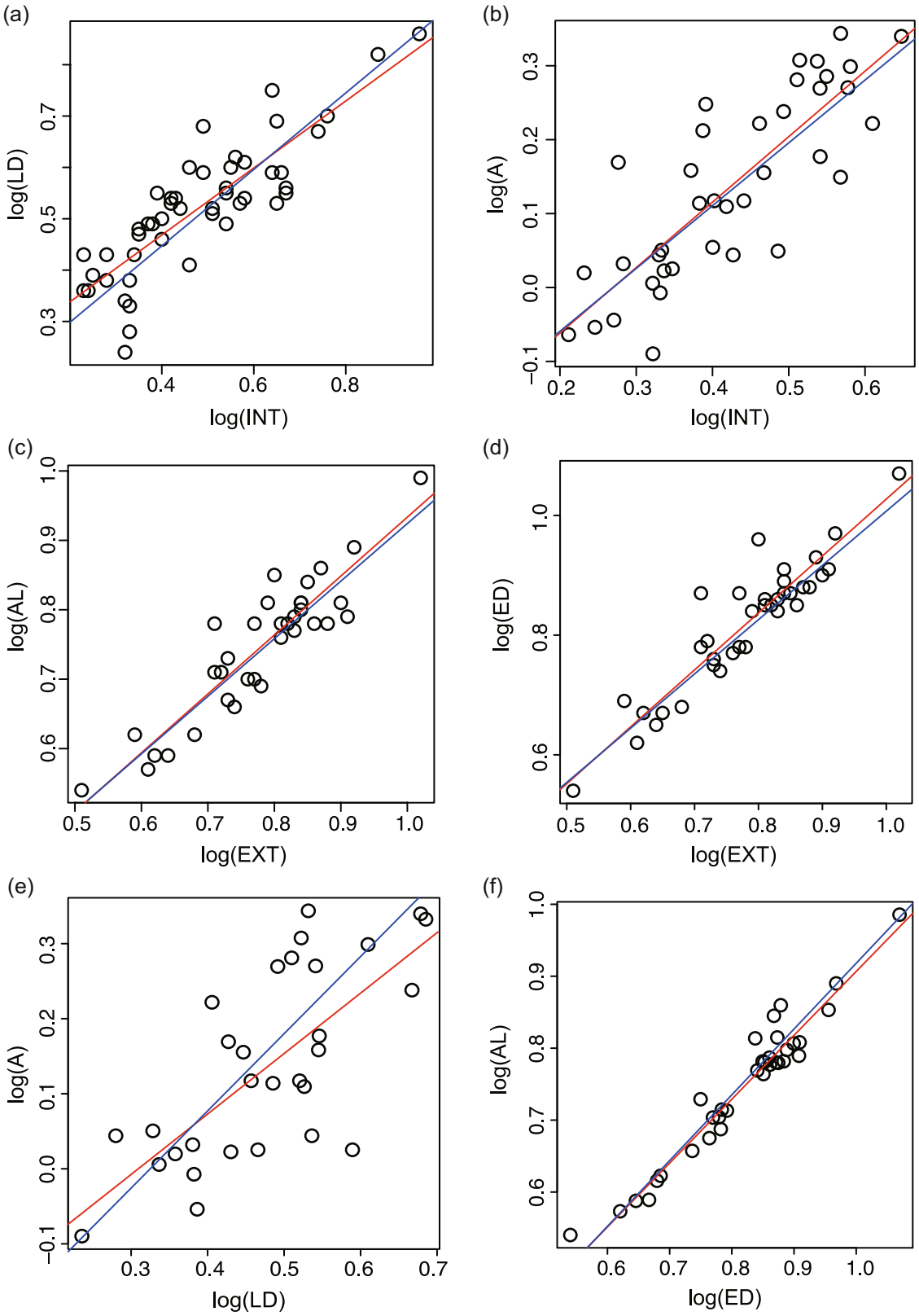

FIGURE 4 Comparison between the regression lines of ordinary least square (OLS; red) and phylogenetic generalized least squares (PGLS; blue). (a) Lens diameter (LD) and internal scleral ossicle ring diameter (INT). (b) Pupil diameter (A) and INT. (c) Axial length (AL) and external scleral ossicle ring diameter (EXT). (d) Eyeball diameter (ED) and EXT. (e) A and LD. (f) AL and ED. All data had been log-transformed before analyses.

4 | DISCUSSION

4.1 | Correlations between soft and hard tissue structures

The strong correlations demonstrated between diameters of the scleral ossicle ring and the soft tissue structures in squamate eyes allow us to predict the sizes of soft tissue structures of an eye in fossil species based on data of the preserved scleral ossicle ring. We tested the precision of the estimation for soft structures using these correlations on one of the measured specimens of extant *A. agama*. The estimated values of the LD (OLS: 3.06 mm, RMA: 3.01 mm, PGLS: 2.92 mm), A (OLS: 1.50 mm, RMA: 1.36 mm, PGLS: 1.36 mm), ED (OLS: 7.41 mm, RMA: 7.38 mm, PGLS: 7.24 mm), AL (OLS: 6.20 mm, RMA: 6.22 mm, PGLS: 6.17 mm) with the internal diameter of the scleral ossicle ring (2.68 mm) and external diameter of the scleral ossicle ring (6.84 mm) were slightly different from the directly measured values of the LD (3.35 mm), A (1.44 mm), ED (7.88 mm), and AL (6.43 mm). However, most of the estimated values fall within the interval of 105%~90% of the measured values, indicating that the estimation of the sizes of soft structures based on that of the scleral ossicle ring is reasonable enough for paleontological applications. Accordingly, the present results will serve as a solid basis for inferring visual performance quantitatively for fossil squamates such as mosasaurs, which often preserve scleral ossicle rings (Daza et al., 2013; Goldfuss, 1845; Konishi et al., 2012; Marsh, 1872, 1880; Russell, 1967; Underwood, 1970; Williston, 1914).

For some nonsquamate taxa, inferences about behavioral patterns in fossil forms have already been made based on correlations between eye structures and behavior in modern animals. One of the commonly used correlations is between the corneal diameter and diurnal or nocturnal activity. In primates, the relative corneal size in diurnal species is significantly smaller than that in nocturnal or cathemeral species (Kirk, 2004). Photopic birds have eyes with larger ALs relative to corneal diameters for improved visual acuity, whereas scotopic birds have eyes with larger corneal diameters relative to ALs for better visual performance (Hall & Ross, 2007). Furthermore, previous studies demonstrated tight correlations in size between these soft tissue structures and skeletal elements associated with the eye in birds and mammals (Kirk, 2006; Schmitz, 2009). Thus, sizes of such skeletal structures associated with the eye may be used for inferring diel activity modes in these taxa (Martin, 1990; Hall, 2008a; 2009; Schmitz, 2009).

A similar correlation between the activity pattern and eye morphology was previously observed in lizards by Werner and Seifan (2006) and Hall (2008a), although the latter author (Hall, 2008a) also noted that skeletal characteristics alone were not sufficient for estimating light-level adaptation in fossil taxa. On the other hand, Atkins and Franz-Odendaal (2016) showed significant correlations between the diel activity patterns (photopic/scotopic) and the ratio between the internal and external diameters of the scleral ossicle ring. This is consistent with the results obtained in the present study: the sizes of the internal and external diameters of the scleral ossicle ring are correlated with the maximum entrance diameter of the pupil and the AL, respectively, both of which significantly affect visual performance. Furthermore, strong correlations among eye structures revealed in this study will allow us to discuss paleoecology of fossil species more accurately through direct reconstruction of their visual performance. For example, diving behavior is correlated with visual performance and eye morphology (Sivak & Millodot, 1977). In deep diving animals, the eye size relative to their body size and the pupil size relative to the eye size tends to become large (Levenson & Schusterman, 1999; D. Marshall, 1953, N. B. Marshall, 1979; Munk & Frederiksen, 1974; Prokofiev, 2014). An eye with a relatively large pupil (low *f*-number) can see an object in the dark and greater water depth. This relationship was previously used for discussion on diving depth in fossil marine reptiles based on the size of the INT (Fernández et al., 2005). However, the comparison of eye sensitivity in Fernández et al. (2005) was limited to a variation within a single clade, Ichthyopterygia. If sensitivity itself can be quantitatively reconstructed, it will be possible to compare behavioral patterns of fossil taxa with those belonging to different clades including modern animals.

It should be noted, however, that diving animals such as cetaceans, pinnipeds, sea turtles, and penguins, in which accommodation is achieved through the motion of the lens only, have a spherical lens, unlike lenticular-shaped one ubiquitously present in terrestrial amniotes (Mass & Supin, 2007; Ott, 2006; Underwood, 1970). Accordingly, caution needs to be exercised in reconstructing the LD of aquatic animals such as mosasaurs although the difference in the shape of the lens between aquatic and terrestrial amniotes seems to have little influence on the inference of the LD based on the internal diameter of the scleral ossicle ring. Furthermore, the strong correlations between soft tissue structures are also possibly useful in reconstructing the eye structures of fossil lizards. For example, Hall (2009) showed strong correlations between the AL and skull structures such as the distance between the left and right orbits and the distance from the ventral margin of the orbit to the midline of the skull roof in extant lizards. By combining these correlations with those between the AL and ED obtained in the present study, it will be possible to reconstruct the ED based on the skull widths. The result of this study therefore will allow us to reconstruct visual performance of fossil squamates and discuss their paleoecological relationships with other taxa.

We should also consider the distortion of fossil specimens in reconstructing the sizes of soft structures based on preserved scleral ossicle rings. Various methods have been proposed to retrodeform two-dimensional or three-dimensional preserved fossil specimens by using a set of liner or angular measurements (Motani, 1997), landmarks (Bolet et al., 2021; Molnar et al., 2012; Tallman et al., 2014), and geometric morphometrics (Angielczyk & Sheets, 2007; Hedrick & Dodson, 2013). Ideally, such retrodeformation should be performed on fossil specimens before applying the correlations between the skeletal and soft tissue structures found in extant squamates.

4.2 | Comparison with bird eyes

It is known that the general structures of the eye are similar between lizards and birds (Land & Nilsson, 2002; Ott, 2006). For avian eyes, Schmitz (2009) showed that there are also strong correlations in size between soft and hard structures. The results of this study demonstrated that the allometric relationships among those structures in lizard eyes are similar to those in avian eyes. For example, the maximum entrance A scales isometrically with the INT in the lizard eye (OLS slope = 0.89), and that of the avian eye is also isometric (OLS slope = 0.91) based on calculation from the relationship between INT and LD, and the one between LD and A (Schmitz, 2009). Similarities between lizards and birds were also found in the relationships between the external diameter of the scleral ossicle ring and the AL, the LD and the maximum entrance A, and the ED and the AL (Schmitz, 2009). These results may not be surprising considering the close similarity in the eye structures between these two clades. The structures and the accommodation mechanism of lizard eyes show the closest similarity to those of avian eyes among extant reptiles. In lizard and avian eyes, scleral ossicles on the boundary between the cornea and the sclera provide sites for attachments of muscles called Crampton's and Brücke's muscles used for accommodation (Walls, 1942). Crampton's muscle is used for corneal accommodation whereas Brücke's muscle is for lenticular accommodation (Walls, 1942). Among other reptiles, turtles also have a ring of scleral ossicles, although their ciliary muscle is not divided into separate parts (Franz-Odendaal, 2020; Ott, 2006; Walls, 1942). The mechanism of accommodation by turtle eyes is also different. That is, the cornea does not participate in accommodation, which is accomplished solely by alternation of the lens (Franz-Odendaal, 2020; Walls, 1942). Crocodiles have no scleral ossicles and use only lenticular accommodation in water and no accommodation on land (Fleishmann et al., 1988; Ott, 2006). The eye of snakes shows many structural peculiarities not present in those of other reptiles. That is, the ophidian eyes have no scleral ossicles nor ciliary muscles (Walls, 1942) and move the spherical lens along the optical axis in accommodation as do aquatic animals (Caprette et al., 2004; Walls, 1942). Accordingly, among reptiles, the similarities in allometric relationships among eye structures between the avian and lizard eyes are consistent with their close similarities in morphology and accommodation mechanism. Correlations between morpho-functional and allometric similarities across taxa suggested herein can be further tested by investigating the relationships in size between eye structures and the scleral ossicle ring in turtles, which have morphology and accommodation mechanism different from those in squamates. In addition, comparative studies on development of the eye among reptiles may provide clues for the structural basis for the allometric similarities observed in this study. So far, such studies have been mostly focused on birds and turtles (Franz-Odendaal, 2006, 2020; Franz-Odendaal & Hall, 2006; Franz-Odendaal & Vickaryous, 2006). Similar researchs on squamate taxa are warranted.

The sole exception for the similar allometric relationships among eye structures between lizards and birds described above, however, is the one between INT and LD, that is, OLS of the former against latter variables showed largely different slopes (0.67 for lizards and 0.97 for birds). The reason for such different allometry remains ambiguous. One possible explanation, however, is the difference in the molecular composition of the lenses between them. The lens is composed mainly of elongated fiber-like cells containing high concentrations of water-soluble, highly stable proteins called crystallins. Two major categories are recognized in these proteins: ubiquitous crystallins and enzyme- or taxon-specific crystallins. The first category contains α, β, and γ crystallins, which are most prevalent in both vertebrate and invertebrate lenses. The latter category includes crystallins (δ, τ, ε, π, ι, and so on), which are restricted to certain groups of vertebrates and evolutionarily have been derived from metabolic enzymes (Wistow & Piatigorsky, 1988). Previous studies have demonstrated differences in the lens crystallin composition not only in taxon-specific crystallins, but also in enzyme crystallins, between birds and lizards (De Jong et al., 1985; Wistow, 1993). For example, the γ crystallins that are abundant proteins throughout Vertebrata including lizards are absent or in low abundance in avian lenses (Chen et al., 2016; De Jong & Bloemendal, 1981; Harding & Crabbe, 1984). These differences in composition may lead to different optical characteristics to their lenses, thus possibly causing them to show different allometric growth patterns between birds and lizards. Another possible cause of the different allometric growth is an artifact produced by different methods of specimen fixation and measurement of lenses. In this study, specimens of lizard eyes were fixed with 70% ethanol or 10% buffered formalin. However, Schmitz (2009) fixed specimens of avian eyes with Davidson's solution, which is a mixture of 95% ethanol, distilled water, 10% formalin, and glacial acetic acid. As for the measurement of lenses, those of lizards were measured with CT-scan images of stained specimens in the present study whereas those of avian eyes were measured on cross sections of the eyes embedded in paraffin (Schmitz, 2009). These differences of the methods for fixation and measurement might have influenced the comparison of the size of lenses between the two studies.

5 | CONCLUSIONS

This study demonstrated that there are the strong correlations in size between soft and hard structures in squamates eyes. The internal diameter of the scleral ossicle ring was highly correlated with the LD and the maximum entrance A. The external diameter of the scleral ossicle ring was also highly correlated with the AL and the ED. Furthermore, significant correlations were shown between soft structures. These strong correlations will allow us to predict the sizes of soft structures based on those of the hard structures that have been preserved as fossil and reconstruct visual performance in extinct squamates. Such quantitative reconstruction will also make it possible to compare the sensitivity and behavioral patterns between extinct and extant taxa that even belong to different clades.

The allometric relationships between the hard and soft structures, except the internal diameter and the LD, found in lizards herein were similar to those in birds, which share similar features in the eye structure and mode of accommodation. This finding suggest that similar morphology of eyes results in similar allometric patterns across taxa and possibly similar functioning. To test this hypothesis, however, similar investigations on the hard and soft structures in turtles, another extant clade of reptiles possessing osseous sclerotic rings, are crucial.

AUTHOR CONTRIBUTIONS

Momo Yamashita: conceptualization (equal); data curation (equal); formal analysis (equal); funding acquisition (equal); investigation (equal); methodology (equal); project administration (equal); resources (equal); software (equal); supervision (equal); validation (equal); visualization (equal); writing—original draft (equal); writing—review and editing (equal). **Takanobu Tsuihiji**: conceptualization (equal); data curation (equal); formal analysis (equal); investigation (equal); methodology (equal); project administration (equal); supervision (equal); validation (equal); writing—original draft (equal); writing—review and editing (equal).

ACKNOWLEDGMENTS

We would like to thank Kazuyoshi Endo, Takenori Sasaki, and Hideki Endo (The University of Tokyo) for many helpful comments throughout this project. Thanks are also due to Tai Kubo for his advices on the PGLS analysis. We would also like to thank the following people and institutions for access to various specimens: Alan Resetar and Tan Fui-Lian (The Field Museum); Tsuyosi Shirawa (iZoo). Momo Yamashita would also like to thank Masahumi Murayama, Yuji Yamamoto, and Takuya Matsuzaki (Center for Advanced Marine Core Research) for her use of the CT scan facility under their care. We are particularly grateful to Makoto Manabe (National Museum of Nature and Science) for access to specimens and CT scan facility under his care, as well as for his advice, during this project. This study was supported by of JSPS KAKENHI (15J10919), as well as by Yoshihiro Kudoh, M. Tanimoto, Toshiharu Mitsuhashi, Masao Nagakawa, Kazuo Takahashi, and 37 others supporters via the academic crowdfunding platform "Academist" (both to Momo Yamashita).

DATA AVAILABILITY STATEMENT

The authors confirm that the data supporting the findings of this study are available within the article.

ORCID

Momo Yamashita http://orcid.org/0000-0003-0151-6378

REFERENCES

Angielczyk, K. D., & Sheets, H. D. (2007). Investigation of simulated tectonic deformation in fossils using geometric morphometrics. *Paleobiology*, *33*(1), 125–148.

Martin, G. R. (1990). *Birds by night* (p. 240). T & AD Poyser.

Atkins, J. B., & Franz-Odendaal, T. A. (2016). The sclerotic ring of squamates: an evo-devo-eco perspective. *Journal of Anatomy*, *229*(4), 503–513.

Banks, M. S., Sprague, W. W., Schmoll, J., Parnell, J. A., & Love, G. D. (2015). Why do animal eyes have pupils of different shapes? *Science Advances*, *1*(7), e1500391.

Bolet, A., Stanley, E. L., Daza, J. D., Arias, J. S., Čerňanský, A., Vidal-García, M., Bauer, A. M., Bevitt, J. J., Peretti, A., & Evans, S. E. (2021). Unusual morphology in the mid-Cretaceous lizard Oculudentavis. *Current Biology*, *31*(15), 3303–3314.

Caprette, C. L., Lee, M. S., Shine, R., Mokany, A., & Downhower, J. F. (2004). The origin of snakes (Serpentes) as seen through eye anatomy. *Biological Journal of the Linnean Society*, *81*(4), 469–482.

Chen, Y., Sagar, V., Len, H. S., Peterson, K., Fan, J., Mishra, S., McMurtry, J., Wilmarth, P. A., David, L. L., & Wistow, G. (2016). γ-Crystallins of the chicken lens: Remnants of an ancient vertebrate gene family in birds. *The FEBS journal*, *283*(8), 1516–1530.

Cott, H. B. (1940). *Adaptive coloration in animals* (p. 600). Methuen.

Curtis, E. L., & Miller, R. C. (1938). The sclerotic ring in North American birds. *The Auk*, *55*(2), 225–243.

Daza, J. D., Bauer, A. M., Wagner, P., & Böhme, W. (2013). A reconsideration of *Sphaerodactylus dommeli* Böhme, 1984 (Squamata: Gekkota: Sphaerodactylidae), a Miocene lizard in amber. *Journal of Zoological Systematics and Evolutionary Research*, *51*(1), 55–63.

Dollo, L. (1889). Première note sur les mosasauriens de Mesvin. *Bulletin de la Société Belge de Geologie, de Paleontolgie et d'Hydrologie*, *3*, 271–304.

Edinger, T. (1929). ÜBer knöcherne Scleralringe. *Zoologische Jahrbücher. Abteilung für Systematik Geographie und Biologie der Tiere*, *51*, 163–226.

Fernández, E., Pelayo, F., Romero, S., Bongard, M., Marin, C., Alfaro, A., & Merabet, L. (2005). Development of a cortical visual neuroprosthesis for the blind: The relevance of neuroplasticity. *Journal of Neural Engineering*, *2*(4), R1–R12.

Fleishman, L. J., Howland, H. C., Howland, M. J., Rand, A. S., & Davenport, M. L. (1988). Crocodiles don't focus underwater.*Journal of Comparative Physiology A*, *163*(4), 441–443.

Franz-Odendaal, T. A. (2006). Intramembranous ossification of scleral ossicles in *Chelydra serpentina*. *Zoology*, *109*(1), 75–81.

Franz-Odendaal, T. A. (2008). Scleral ossicles of teleostei: Evolutionary and developmental trends. *The Anatomical Record*, *291*(2), 161–168.

Franz-Odendaal, T. A. (2020). Skeletons of the eye: An evolutionary and developmental perspective. *The Anatomical Record*, *303*(1), 100–109.

Franz-Odendaal, T. A., & Hall, B. K. (2006). Skeletal elements within teleost eyes and a discussion of their homology. *Journal of Morphology*, *267*(11), 1326–1337.

Franz-Odendaal, T. A., & Vickaryous, M. K. (2006). Skeletal elements in the vertebrate eye and adnexa: Morphological and developmental perspectives. *Developmental Dynamics: An Official Publication of the American Association of Anatomists*, *235*(5), 1244–1255.

Freckleton, R. P., Harvey, P. H., & Pagel, M. (2002). Phylogenetic analysis and comparative data: A test and review of evidence. *The American Naturalist*, *160*(6), 712–726.

Gignac, P. M., & Kley, N. J. (2014). Iodine-enhanced micro-CT imaging: Methodological refinements for the study of the soft-tissue anatomy of post-embryonic vertebrates. *Journal of Experimental Zoology Part B: Molecular and Developmental Evolution*, *322*(3), 166–176.

Goldfuss, A. (1845). Der Schädelbau des *Mosasaurus*, durch Beschreibung einer neuen Art dieser Gattung erläutert. *Nova Acta Academa Ceasar Leopoldino-Carolinae Germanicae Natura Curiosorum*, *21*, 1–28.

Gould, S. J. (1966). Allometry and size in ontogeny and phylogeny. *Biological Reviews*, *41*(4), 587–638.

Hall, M. I. (2008a). Comparative analysis of the size and shape of the lizard eye. *Zoology*, *111*(1), 62–75.

Hall, M. I. (2008b). The anatomical relationships between the avian eye, orbit and sclerotic ring: Implications for inferring activity patterns in extinct birds. *Journal of Anatomy*, *212*(6), 781–794.

Hall, M. I. (2009). The relationship between the lizard eye and associated bony features: A cautionary note for interpreting fossil activity patterns. *The Anatomical Record*, *292*(6), 798–812.

Hall, M. I., Iwaniuk, A. N., & Gutiérrez-Ibáñez, C. (2009). Optic foramen morphology and activity pattern in birds. *The Anatomical Record*, *292*(11), 1827–1845.

Hall, M. I., & Ross, C. F. (2007). Eye shape and activity pattern in birds. *Journal of Zoology*, *271*(4), 437–444.

Harding, J. J., & Crabbe, M. J. C. (1984). The lens: Development, proteins, metabolism and cataract. In H. Davson (Ed.), *The eye* (pp. 207–492). Academic Press.

Harmon, L. J., Weir, J. T., Brock, C. D., Glor, R. E., & Challenger, W. (2008). Geiger: Investigating evolutionary radiations. In K Crandall (Ed.), *Bioinformatics* (Vol. 24, 1, pp. 129–131). Oxford Academic.

Harvey, P. H., & Pagel, M. D. (1991). *The comparative method in evolutionary biology* (Vol. 239, p. 248). Oxford University Press.

Hedrick, B. P., & Dodson, P. (2013). Lujiatun psittacosaurids: Understanding individual and taphonomic variation using 3D geometric morphometrics. *PLoS One*, *8*(8), e69265.

Heskes, T. (1996). Practical confidence and prediction intervals. *Advances in Neural Information Processing Systems*, *9*, 176–182.

Huxley, A. (1932). *Problems of relative growth* (p. 276). The Dial Press.

De Jong, W. W., & Bloemendal, H. (1981). Evolution of lens and crystallins. In H. Bloemendal (Ed.), *Molecular and cellular biology of the eye lens* (pp. 221–278). Wiley-Interscience.

De Jong, W. W., Zweers, A., Versteeg, M., Dessauer, H. C., & Goodman, M. (1985). alpha-Crystallin A sequences of *Alligator mississippiensis* and the lizard *Tupinambis teguixin*: Molecular evolution and reptilian phylogeny. *Molecular Biology and Evolution*, *2*(6), 484–493.

Kay, R. F., & Cartmill, M. (1977). Cranial morphology and adaptations of *Palaechthon nacimienti* and other Paromomyidae (Plesiadapoidea,? Primates), with a description of a new genus and species. *Journal of Human Evolution*, *6*(1), 19–53.

Kay, R. F., & Kirk, E. C. (2000). Osteological evidence for the evolution of activity pattern and visual acuity in primates. *American Journal of Physical Anthropology: The Official Publication of the American Association of Physical Anthropologists*, *113*(2), 235–262.

Kirk, E. C. (2004). Comparative morphology of the eye in primates. *The Anatomical Record*, *281*(1), 1095–1103.

Kirk, E. C. (2006). Effects of activity pattern on eye size and orbital aperture size in primates. *Journal of Human Evolution*, *51*(2), 159–170.

Konishi, T., Lindgren, J., Caldwell, M. W., & Chiappe, L. (2012). *Platecarpus tympaniticus* (Squamata, Mosasauridae): Osteology of an exceptionally preserved specimen and its insights into the acquisition of a streamlined body shape in mosasaurs. *Journal of Vertebrate Paleontology*, *32*(6), 1313–1327.

Land, M. F. (1981). Optics of the eyes of *Phronima* and other deep-sea amphipods. *Journal of Comparative Physiology*, *145*(2), 209–226.

Land, M. F., & Nilsson, D. -E. (2002). *Animal Eyes* (p. 121). Oxford University Press.

Legendre, P. (2011). *lmodel2: Model II regression. R package version 1.7–0*. http://CRAN.R-project.org/package=lmodel2

Levenson, D. H., & Schusterman, R. J. (1999). Dark adaptation and visual sensitivity in shallow and deep-diving pinnipeds. *Marine Mammal Science*, *15*(4), 1303–1313.

Loyau, A., Gomez, D., Moureau, B., Théry, M., Hart, N. S., Jalme, M. S., Bennett, A. T. D., & Sorci, G. (2007). Iridescent structurally based coloration of eyespots correlates with mating success in the peacock. *Behavioral Ecology*, *18*(6), 1123–1131.

Loyau, A., Jalme, M. S., & Sorci, G. (2005). Intra-and intersexual selection for multiple traits in the peacock (*Pavo cristatus*). *Ethology*, *111*(9), 810–820.

Luria, S. M., & Kinney, J. A. S. (1970). Underwater vision. *Science*, *167*(3924), 1454–1461.

Maddison, W. P., & Maddison, D. R. (2018). *Mesquite: a modular system for evolutionary analysis Version 3.51*. http://www.mesquiteproject.org

Malmström, T., & Kröger, R. H. (2006). Pupil shapes and lens optics in the eyes of terrestrial vertebrates. *Journal of Experimental Biology*, *209*(1), 18–25.

Marsh, O. C. (1872). Discovery of the dermal scutes of mosasaurid reptiles. *American Journal of Science*, *16*, 290–292.

Marsh, O. C. (1880). New characters of mosasauroid reptiles. *American Journal of Science*, *109*, 83–87.

Marshall, D. (1953). Glioma of the optic nerve as a manifestation of von Recklinghausen's disease. *Transactions of the American Ophthalmological Society*, *51*, 117–155.

Marshall, N. B. (1979). *Developments in deep-sea biology* (p. 566). Blandford Press.

Martin, G. R. (1982). An owl's eye: Schematic optics and visual performance in *Strix aluco* L. *Journal of Comparative Physiology*, *145*(3), 341–349.

Martin, G. R. (1983). Schematic eye models in vertebrates. In D. Ottoson, H. Autrum, E. R. Perl, R. F. Schmidt, H. Shimazu, & W. D. Willis (Eds.), *Progress in sensory physiology* (Vol. 4, pp. 43–81). Springer.

Martin, G. R., & Brooke, M. D. L. (1991). The eye of a procellariiform seabird, the Manx shearwater, *Puffinus puffinus*: Visual fields and optical structure. *Brain, Behavior and Evolution*, *37*(2), 65–78.

Mass, A. M., & Supin, A. Y. (2007). Adaptive features of aquatic mammals' eye. *The Anatomical Record*, *290*(6), 701–715.

Molnar, J. L., Pierce, S. E., Clack, J. A., & Hutchinson, J. R. (2012). Idealized landmark-based geometric reconstructions of poorly preserved fossil material: A case study of an early tetrapod vertebra. *Palaeontologia Electronica*, *15*(1), 1–18.

Motani, R. (1997). New technique for retrodeforming tectonically deformed fossils, with an example for ichthyosaurian specimens. *Lethaia*, *30*(3), 221–228.

Motani, R., Rothschild, B. M., & Wahl, Jr. W. (1999). Large eyeballs in diving ichthyosaurs. *Nature*, *402*(6763), 747.

Munk, O., & Frederiksen, R. D. (1974). On the function of aphakic apertures in teleosts. *Videnskabelige meddelelser fra Dansk naturhistorisk forening i København*, *137*, 65–94.

Orme, D., Freckleton, R., Thomas, G., Petzoldt, T., Fritz, S., Isaac, N., & Pearse, W. (2013). *The caper package: Comparative analysis of phylogenetics and evolution in R. R package version* (Vol. 5, 2, pp. 1–36). R Development Core Team.

Ott, M. (2006). Visual accommodation in vertebrates: mechanisms, physiological response and stimuli. *Journal of Comparative Physiology A*, *192*(2), 97–111.

Pagel, M. (1999). Inferring the historical patterns of biological evolution. *Nature*, *401*(6756), 877–884.

Paradis, E., Claude, J., & Strimmer, K. (2004). APE: Analyses of Phylogenetics and evolution in R language, *Bioinformatics* (Vol. 20, 2, pp. 289–290). Oxford Academic.

Pauwels, E., Van Loo, D., Cornillie, P., Brabant, L., & Van Hoorebeke, L. (2013). An exploratory study of contrast agents for soft tissue visualization by means of high resolution X-ray computed tomography imaging. *Journal of Microscopy*, *250*(1), 21–31.

Pettigrew, J. D., Collin, S. P., & Ott, M. (1999). Convergence of specialised behaviour, eye movements and visual optics in the sandlance (Teleostei) and the chameleon (Reptilia). *Current Biology*, *9*(8), 421–424.

Pilgrim, B. L., & Franz-Odendaal, T. A. (2009). A comparative study of the ocular skeleton of fossil and modern chondrichthyans. *Journal of Anatomy*, *214*(6), 848–858.

Pinheiro, J., Bates, D., DebRoy, S., Sarkar, D., Heisterkamp, S., Van Willigen, B., & Maintainer, R. (2017). Package 'nlme': Linear and nonlinear mixed effects models, version 3. *Scientific Research*, 1–117.

Plisnier-Ladame, F., & Coupatez, P. (1969). Étude morphologique de l'anneau sclrotique de *Mosasaurus hoffmanni* Mantell 1829. *Bulletin Belgische Vereniging Geologie Paleontologie Hydrologie*, *78*, 253–265.

Prokofiev, A. M. (2014). Deepsea herrings (Bathyclupeidae) of the northwestern Pacific ocean. *Journal of Ichthyology*, *54*(2), 137–145.

Revell, L. J. (2012). phytools: An R package for phylogenetic comparative biology (and other things). *Methods in Ecology and Evolution*, *3*(2), 217–223.

Russell, D. A. (1967). Systematics and morphology of American mosasaurs, *Peabody Museum of Natural History Bulletin* (Vol. 23, p. 240). Yale University.

Schmitz, L. (2009). Quantitative estimates of visual performance features in fossil birds. *Journal of Morphology*, *270*(6), 759–773.

Schmitz, L., & Motani, R. (2010). Morphological differences between the eyeballs of nocturnal and diurnal amniotes revisited from optical perspectives of visual environments. *Vision Research*, *50*(10), 936–946.

Schmitz, L., & Motani, R. (2011). Nocturnality in dinosaurs inferred from scleral ring and orbit morphology. *Science*, *332*(6030), 705–708.

Schneider, C. A., Rasband, W. S., & Eliceiri, K. W. (2012). NIH Image to ImageJ: 25 years of image analysis. *Nature Methods*, *9*(7), 671–675.

Sivak, J. G., & Millodot, M. (1977). Optical performance of the penguin eye in air and water. *Journal of Comparative Physiology*, *119*(3), 241–247.

Sokal, R. R., & Rohlf, F. J. (1995). *Biometry* (3rd ed., p. 887). W.H. Freeman and Company.

Tallman, M., Amenta, N., Delson, E., Frost, S. R., Ghosh, D., Klukkert, Z. S., Morrow, A., & Sawyer, G. J. (2014). Evaluation of a new method of fossil retrodeformation by algorithmic symmetrization: Crania of papionins (Primates, Cercopithecidae) as a test case. *PLoS One*, *9*(7), e100833.

Thewissen, J. G., & Nummela, S. (2008). *Sensory evolution on the threshold: Adaptations in secondarily aquatic vertebrates* (p. 351). University of California Press.

Underwood, G. (1970). The eye. In C. Gans, & T. S. Parsons (Eds.), *Biology of the reptilia* (pp. 1–97). Academic Press.

Vickerton, P., Jarvis, J., & Jeffery, N. (2013). Concentration-dependent specimen shrinkage in iodine-enhanced micro CT. *Journal of Anatomy*, *223*(2), 185–193.

Walls, G. L. (1942). *The vertebrate eye and its adaptive radiation* (p. 785). Cranbrook Institute of Science.

Warrant, E. J., & Locket, N. A. (2004). Vision in the deep sea. *Biological Reviews*, *79*(3), 671–712.

Warton, D. I., Duursma, R. A., Falster, D. S., & Taskinen, S. (2012). matr 3–An R package for estimation and inference about allometric lines. *Methods in Ecology and Evolution*, *3*(2), 257–259.

Werner, Y. L., & Seifan, T. (2006). Eye size in geckos: Asymmetry, allometry, sexual dimorphism, and behavioral correlates. *Journal of Morphology*, *267*(12), 1486–1500.

Williston, S. W. (1914). *Water Reptiles of the Past and Present* (p. 251). University of Chicago Press.

Wistow, G. (1993). Lens crystallins: Gene recruitment and evolutionary dynamism. *Trends in Biochemical Sciences*, *18*(8), 301–306.

Wistow, G. J., & Piatigorsky, J. (1988). Lens crystallins: The evolution and expression of proteins for a highly specialized tissue. *Annual Review of Biochemistry*, *57*(1), 479–504.

Wong, M. D., Spring, S., & Henkelman, R. M. (2013). Structural stabilization of tissue for embryo phenotyping using micro-CT with iodine staining. *PLoS One*, *8*(12), e84321.

Zheng, Y., & Wiens, J. J. (2016). Combining phylogenomic and supermatrix approaches, and a time-calibrated phylogeny for squamate reptiles (lizards and snakes) based on 52 genes and 4162 species. *Molecular Phylogenetics and Evolution*, *94*, 537–547.

SUPPORTING INFORMATION

Additional supporting information can be found online in the Supporting Information section at the end of this article.

How to cite this article: Yamashita, M., & Tsuihiji, T. (2022). The relationship between hard and soft tissue structures of the eye in extant lizards. *Journal of Morphology*, *283*(9), 1182–1199. https://doi.org/10.1002/jmor.21495